sustainability

MDPI

Article

Degradation of Carbamazepine by Ozonation: Influence of pH and Mass Transfer on Water Quality Improvement for Sustainable Water Treatment

Marco Antonio Villagómez-Cuéllar [1], Elisabeth Bilbao-García [1], Unai Duoandicoechea [2] and Natalia Villota [2,*]

[1] Department of Environmental and Chemical Engineering, Bilbao School of Engineering, University of the Basque Country UPV/EHU, 48013 Bilbao, Spain; marco.villagomez@gmail.com (M.A.V.-C.); elisabeth.bilbao@ehu.eus (E.B.-G.)

[2] Department of Environmental and Chemical Engineering, Faculty of Engineering Vitoria-Gasteiz, University of the Basque Country UPV/EHU, Nieves Cano 12, 01006 Vitoria-Gasteiz, Spain; unai.duoandicoechea@ehu.eus

* Correspondence: natalia.villota@ehu.eus; Tel.: +34-945013248

Abstract

The presence of persistent pharmaceutical contaminants such as carbamazepine in aquatic environments represents a major challenge for sustainable water management and the long-term protection of water resources. Carbamazepine (CBZ) is a persistent pharmaceutical pollutant frequently detected in surface waters and poorly removed in conventional wastewater treatment plants. This study investigates the ozonation of CBZ (50.0 mg/L) under alkaline conditions (pH 10.0–14.0), focusing on the influence of pH and ozone mass transfer on oxidation kinetics and water-quality parameters. Ozonation was conducted at 25 °C using a high ozone dose (58.5 g Nm^{-3}), achieving complete CBZ degradation within the first 10 min at all pH values. Marked differences in pH evolution were observed: solutions initially at pH 10.1 rapidly acidified to pH ≈ 4.0, whereas highly alkaline systems (pH > 13.0) remained stable. The most intense yellow coloration was observed at pH 14.0, followed by progressive removal. Turbidity remained low at pH 10.1 (<2.5 NTU) but increased at pH 12.0–13.0. Ozone mass-transfer behaviour revealed a transition from molecular-ozone-dominated oxidation to radical-dominated regimes at pH ≥ 12.0. Overall, ozonation proves highly efficient for CBZ removal, and the pH-dependent behaviour highlights the need to optimise oxidation conditions to improve water quality and minimise residual by-products, thereby supporting the development of more sustainable advanced treatment strategies for wastewater reuse and environmental protection.

Keywords: advanced oxidation processes (AOPs); carbamazepine (CBZ); colour; ozonation; emerging contaminants; microcontaminants; pH; sustainability; sustainable water treatment; turbidity; wastewater reuse

Check for updates

Academic Editor: José Alberto Herrera-Melián

Received: 27 March 2026
Revised: 16 April 2026
Accepted: 23 April 2026
Published: 24 April 2026

Copyright: © 2026 by the authors. Licensee MDPI, Basel, Switzerland. This article is an open access article distributed under the terms and conditions of the Creative Commons Attribution (CC BY) license.

1. Introduction

In recent decades, increasing attention has been directed toward the presence of compounds in water bodies that were not previously considered hazardous, both in terms of their distribution and concentration. Advances in analytical techniques have enabled the detection of many substances that had gone unnoticed and are now recognised as capable of causing adverse effects on ecosystems and human health [1]. These substances are collectively referred to as emerging contaminants (ECs), a broad group that includes both organic

(biodegradable and non-biodegradable) and inorganic compounds (heavy metals, nitrates, phosphates, etc.). Their presence in aquatic environments is closely associated with the growth of the pharmaceutical and personal care product industries, intensive agricultural activities, and various industrial processes. Common examples include pharmaceuticals (e.g., antibiotics, anti-inflammatories), cosmetics, pesticides, surfactants, plasticisers such as bisphenols and phthalates, and food additives.

The widespread consumption of pharmaceuticals has resulted in their continuous introduction into wastewater treatment plants (WWTPs). However, conventional WWTPs often lack the capacity to effectively remove these compounds, leading to their recurrent detection in surface waters [2]. Many pharmaceuticals and personal care products also act as endocrine-disrupting compounds (EDCs), posing risks to aquatic organisms, ecosystems and public health. Despite this, traditional wastewater treatment processes exhibit limited efficiency in removing these contaminants [3].

From a sustainability perspective, the insufficient removal of pharmaceutical contaminants in conventional wastewater treatment plants compromises environmental quality, water reuse potential and compliance with sustainable development goals related to clean water and sanitation. The development and optimisation of advanced treatment technologies capable of efficiently removing recalcitrant micropollutants are therefore essential to support sustainable wastewater management, protect aquatic ecosystems and enable safe water reuse.

To address these challenges, various strategies have been explored for EC removal. Physical methods include adsorption (activated carbon, biochar, carbon nanotubes), membrane filtration (microfiltration, ultrafiltration, reverse osmosis), sedimentation, and aeration. Chemical and advanced approaches include advanced oxidation processes (AOPs), ozonation, peroxide-based oxidation, electrochemical oxidation, coagulation–flocculation, and photocatalysis with materials such as TiO_2 and WO_3. However, no single treatment method has demonstrated universal efficiency across all ECs, encouraging the development of hybrid technologies that combine physical and chemical processes to enhance removal performance.

This study focuses on the removal of carbamazepine (CBZ), a widely prescribed antiepileptic and mood-stabilising pharmaceutical used to treat neurological conditions such as epilepsy, depression and bipolar disorder. In humans, approximately 72% of CBZ is absorbed and metabolised in the liver, while the remaining 28% is excreted in faeces. CBZ is produced globally in large quantities and is known for its environmental persistence; its metabolites and degradation products are biologically active and resistant to natural attenuation. Reported half-lives range from 84 to 2100 h under solar radiation and from 3000 to 5100 h in river water [4]. Major metabolites detected in urine include CBZ-epoxide, CBZ-diol, CBZ-acridane, 2-OH-CBZ and 3-OH-CBZ. Due to its physicochemical properties, CBZ is considered a recalcitrant contaminant with demonstrated low removal efficiency in conventional water treatment systems [5,6].

CBZ ecotoxicity has been documented across various aquatic species, with several studies reporting effective concentration (EC_{50}) values related to developmental, reproductive or survival impacts. Reported values include: Alivibrio fischeri EC_{50} = 64.2 mg/L (30 min) [7], Chlorella vulgaris EC_{50} = 110.9 mg/L (24 h) [8], and Danio rerio EC_{50} = 85.6 mg/L (3 days) [9], with lethality reported in Daphnia magna (LC_{50} = 111 mg/L after 48 h). Potential risks to humans have also been highlighted, including associations with spina bifida, foetal neurological development issues [10], increased foetal loss and higher malformation rates in pregnant women [11].

Although CBZ attenuation in aquatic systems can occur through natural mechanisms such as photolysis, aerobic biodegradation, adsorption onto sediments, and dilution in

water bodies [12], these processes are generally slow and incomplete. Its physicochemical profile, characterised by an octanol–water partition coefficient (Log K_ow) between 0 and 4.5 [13], identifies CBZ as moderately hydrophilic, facilitating its mobility and persistence in surface waters [14,15]. For instance, CBZ concentrations of 41.6 ng/mg have been reported in sediments from 44 rivers in the United States [16].

The primary source of CBZ in surface waters is the discharge of effluents from WWTPs [17], with additional inputs arising from stormwater runoff carrying municipal and hospital waste [18]. CBZ can also accumulate in soils irrigated with reclaimed wastewater or amended with sewage sludge [19], and it has been detected in marine environments due to surface runoff and direct discharge. Concentrations in freshwater systems vary widely, from 0.1–34.7 ng/L in Japan to 2–172 ng/L in the United States and 9–327 ng/L in the United Kingdom, with values exceeding 1000 ng/L in Berlin. Notably, CBZ can persist for more than eight years in subsurface environments without significant degradation [20]. Moreover, incomplete oxidation during conventional treatments can yield toxic by-products such as acridine under sunlight exposure [21]. Due to its persistence and limited removal, CBZ is widely used as a chemical indicator of anthropogenic pollution in surface waters [22,23].

Multiple studies confirm that CBZ removal efficiencies in WWTPs are typically below 10%, attributed to its low biodegradability and weak tendency to adsorb to sludge. Among the advanced oxidation processes investigated for CBZ degradation, ozone-based systems (O_3, O_3/H_2O_2, O_3/UV) and UV/H_2O_2 have shown the greatest potential, generating reactive oxygen species capable of oxidising persistent pharmaceutical contaminants [24,25]. However, the efficiency of ozonation depends strongly on operational parameters such as pH, ozone concentration, and mass transfer characteristics.

Previous studies have reported highly variable degradation efficiencies for CBZ during ozonation, depending on operating conditions such as pH, initial pollutant concentration and ozone dose. Darabi et al. (2024) observed CBZ removal efficiencies ranging from 21% at pH 5, 66% at pH 7, and up to 81% at pH 11 during pure ozonation, reaching 78% removal when increasing the injected ozone dose from 200 to 400 mg/h and achieving up to 100% degradation within 180 s at the highest ozone exposure conditions [24]. In another study evaluating the coupling of ozonation and nanofiltration, complete CBZ degradation was achieved within 5 min of ozonation, although mineralisation remained limited (<12%). Catalytic ozonation studies have similarly reported complete transformation of CBZ within the first minutes of treatment, even though some aromatic intermediates exhibit slower decomposition [25,26]. These results consistently highlight that CBZ is highly susceptible to rapid oxidative breakdown by ozone, although the extent of degradation and persistence of by-products strongly depend on the oxidation regime and operational conditions.

Therefore, the present study aims to investigate the degradation behaviour of carbamazepine during ozonation and to provide mechanistic insights that support the optimisation of ozonation-based advanced oxidation processes for sustainable wastewater treatment and water quality improvement, focusing specifically on the influence of pH and gas–liquid mass transfer on both oxidation efficiency and water quality improvement. By analysing colour formation, turbidity changes and dissolved ozone dynamics, this work seeks to deepen the understanding of CBZ ozonation pathways and to provide insights relevant for the optimisation of advanced treatment processes in wastewater management.

Despite the extensive literature on CBZ ozonation and the well-known influence of pH on ozone decomposition pathways, important knowledge gaps remain regarding the interplay between alkalinity, ozone stability and gas–liquid mass transfer dynamics during CBZ oxidation. Existing studies have typically focused either on degradation kinetics or on the identification of transformation products, but rarely on the fundamental processes

that modulate the transition between molecular-ozone and radical-driven regimes. As a result, the mechanistic implications of pH for ozone availability, intermediate formation and overall water-quality evolution are still not fully understood.

In this context, the present work provides a comprehensive mechanistic assessment of CBZ ozonation by simultaneously monitoring ozone in both gas and liquid phases, pH evolution, aromaticity, colour and turbidity. This integrative approach enables the identification of distinct oxidation regimes as alkalinity increases and reveals how pH governs not only the oxidation pathway but also the transient formation and persistence of coloured and particulate intermediates. Unlike previous studies that primarily describe CBZ removal, the present research highlights the strong pH-dependent behaviour of water-quality indicators, demonstrating that complete CBZ degradation does not necessarily correlate with improved aesthetic or physicochemical properties of the treated water.

Furthermore, this study introduces a novel quantitative evaluation of the volumetric ozone mass-transfer coefficient (k_{La}) under varying initial pH conditions, elucidating how the chemical instability of ozone at high alkalinity affects its capacity to accumulate in solution. By establishing the link between pH-driven ozone decomposition, apparent mass-transfer behaviour and the formation of transformation products, the work provides new insights that are essential for designing and optimising ozonation-based advanced oxidation processes. These contributions extend the current understanding of CBZ oxidation and support the development of treatment strategies that balance rapid contaminant removal with effective control of water-quality outcomes.

In contrast to most previous CBZ ozonation studies, which primarily report removal efficiencies or transformation product identification, the present work systematically links pH-dependent ozone stability, gas–liquid mass transfer and water-quality indicators within a single experimental framework. By explicitly distinguishing molecular-ozone-dominated and radical-dominated oxidation regimes and quantifying their impact on colour, turbidity and aromaticity, this study provides mechanistic insight that goes beyond CBZ disappearance and addresses critical limitations of earlier ozonation studies.

2. Materials and Methods

Ozonation experiments were carried out using a laboratory-scale semi-continuous system (see Figure 1) specifically designed to bring ozone (O_3) into controlled contact with liquid samples. Carbamazepine (CBZ) solutions with an initial concentration of $[CBZ]_0$ = 50.0 mg/L were prepared by dissolving analytical-grade CBZ (Fagron, Rotterdam, The Netherlands, 99.1%) in distilled water using a glass beaker. A CBZ concentration of 50.0 mg/L was intentionally selected to ensure accurate mechanistic analysis of ozonation. Environmentally relevant concentrations (ng/L–µg/L) are below the detection limits of HPLC–UV for identifying transient intermediates and do not produce measurable changes in ozone decay, pH evolution, colour, or turbidity. Using a higher concentration enables clear observation of reaction pathways, mass-transfer effects, and pH-dependent shifts between molecular-ozone and radical oxidation regimes. This approach is standard in mechanistic AOP research and is not intended to reproduce real wastewater concentrations but to provide controlled, reproducible conditions for understanding the fundamental chemistry of CBZ ozonation.

The ozonation reactions were conducted in a 1 L semi-continuous reactor equipped with four ports accommodating the pH electrode HI2003 (Hanna Instruments Edge, Woonsocket, RI, USA), the dissolved ozone electrode of the DOZ6000 Controller Dissolved Ozone Meter (Chemtrac Inc., Norcross, GA, USA), and the ozone gas injector. The ozone concentration in the gas phase was monitored using an Ozone Analyzer BMT 964C—Ozone Content (Ozone Solutions Inc., Hull, IA, USA). The initial pH was adjusted with a few drops

of concentrated HCl or NaOH to avoid dilution effects. The solutions were kept under constant stirring at 500 rpm until complete homogenisation. Due to the slow dissolution rate of CBZ, each solution was prepared 24 h prior to its respective experimental run.

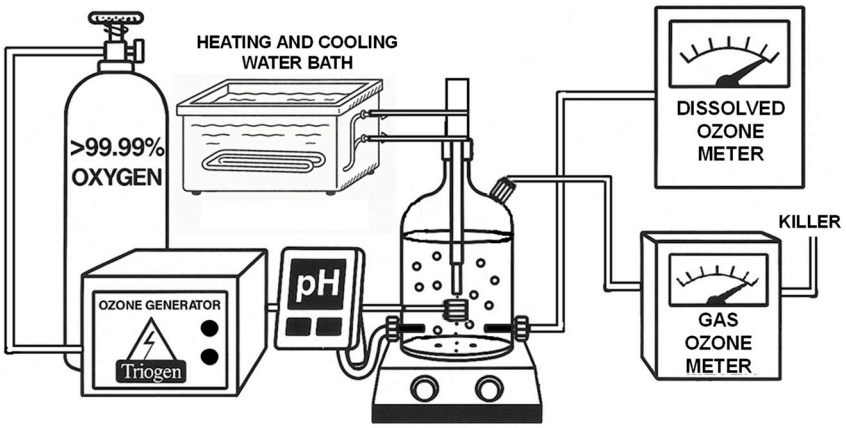


Figure 1. Laboratory-scale ozonation system.

Ozone was generated from high-purity oxygen (≥99.999%; Air Liquide, Madrid, Spain) using a Triogen LAB2B corona discharge generator (BIO-UV Group, Lunel, France). The gas stream was introduced into the reactor through a silicon carbide micro-diffuser placed at the base. The reactor contains an internal quartz sleeve through which water is recirculated using an insulated thermostatic bath (Frigiterm-P, Selecta, Barcelona, Spain) to maintain the system at 25 °C. The applied ozone gas flow rate was measured and regulated at 1 L/min using a Vogueing YB-4M control valve.

To maximise ozone solubilisation and enhance its decomposition into hydroxyl radicals, additional ozone was introduced through a Pawfly ASC-025 micro-diffuser (Aipade, Shenzhen, China) composed of high-temperature sintered porous mineral stone. The system also incorporates an ozone destructor to remove residual ozone before venting to the atmosphere, preventing the release of this toxic and corrosive gas.

The influence of pH on the ozonation process was assessed by conducting experiments under different initial pH values ($[pH]_0$ = 10.0–14.0) while applying a high ozone concentration in the gas phase ($[O_3]$gas = 58.5 g/Nm^3). These conditions were selected because previous experimental observations confirmed that they promote the formation of yellow coloration and turbidity in CBZ aqueous solutions during ozonation.

Control experiments were performed at all initial pH values (10–14) in the absence of ozone in order to confirm that CBZ does not undergo chemical transformation under alkaline conditions alone. In these ozone-free tests, CBZ concentrations remained constant throughout the entire experimental period, demonstrating that neither hydrolysis nor any other pH-driven chemical degradation pathway occurs under the conditions used. Therefore, the disappearance of CBZ observed during the ozonation experiments can be unequivocally attributed to the oxidative action of molecular ozone and its radical by-products, and not to any parallel abiotic transformation process.

The concentration of CBZ was determined using High-Performance Liquid Chromatography (Model 2695, Waters Chromatography S.A., Cerdanyola del Vallès, Spain) equipped with a Dual λ absorbance detector (Model 2487, Waters Chromatography S.A., Cerdanyola del Vallès, Spain). The analyses were performed using a Zorbax Eclipse PAH column (150 mm × 4.6 mm, particle size 5 µm) together with a Zorbax Eclipse PAH guard column (4.6 mm × 12.5 mm), both supplied by Agilent (Santa Clara, CA, USA). The mobile phase consisted of water and acetonitrile (ACN), with a flow rate of 0.8 mL/min. The initial gradient started at 20% ACN, increased to 45% *v*/*v* in 3 min, was held for 6 min, and then

decreased back to 20% *v*/*v* in 1 min. The total run time was 10 min, with an injection volume of 50 µL, and all separations were performed at room temperature. CBZ identification was achieved by comparing retention times with a standard, and detection was performed at 275 nm. The turbidity of the samples was analysed by a nephelometric turbidimeter (model HI88703, Hanna Instruments S.L., Eibar, Spain). This instrument quantifies turbidity by detecting the intensity of light scattered at 90° by suspended particles in the water sample. Measurements were expressed in NTU (Nephelometric Turbidity Units), the standard unit defined by ISO 7027 [27] and USEPA Method 180.1 for turbidity analysis. The colour and aromaticity were measured with a UV–Vis spectrophotometer (model V-630, Jasco, Madrid, Spain) at 455 and 254 nm, respectively.

3. Results

3.1. Kinetics of CBZ Ozonation

Figure 2 illustrates the kinetics of carbamazepine (CBZ) ozonation under optimal process conditions, showing complete CBZ degradation within the first 10 min of reaction, regardless of the operating pH. This behaviour indicates that, under the high ozone concentration used (58.5 g/Nm^3), the oxidation rate is mainly controlled by the high availability of ozone and not by the pH of the medium, which allows the initial degradation of CBZ to be very rapid across the entire basic range studied.

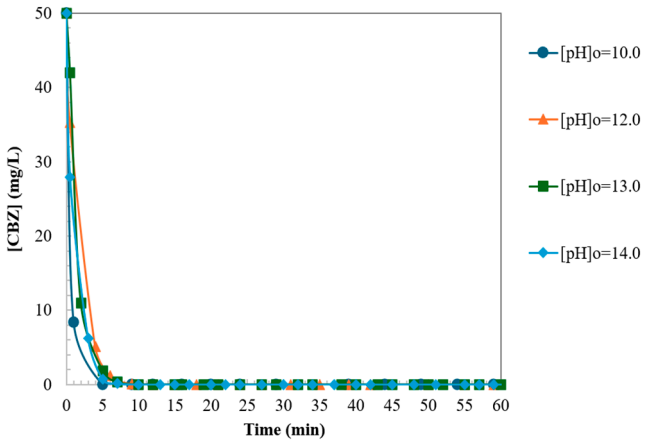


Figure 2. Kinetic degradation of CBZ during ozonation treatment. Experimental conditions: $[CBZ]_0$ = 50.0 mg/L; [T] = 25 °C; $[O_3]_{gas}$ = 58.5 g/Nm^3.

The possibility of alternative chemical transformation pathways contributing to CBZ removal was examined and explicitly excluded. CBZ is known to be highly resistant to hydrolysis and does not undergo degradation in strongly alkaline media in the absence of oxidants. This was confirmed experimentally through ozone-free controls, in which no decrease in CBZ concentration was observed. The kinetic profiles of ozone in both the gas and liquid phases, together with the pH evolution and changes in aromaticity, colour, and turbidity, all point consistently to ozonation—via direct molecular attack at moderate alkalinity and via hydroxyl radical formation at high pH—as the only operative mechanism. Hence, the results presented reflect exclusively ozone-driven oxidation processes, with high pH acting solely as a modulator of the oxidative regime rather than introducing any competing degradation pathways.

The near overlap of the kinetic curves at all evaluated pH values indicates that, under these conditions, the limiting stage of the process is not the activation of ozone or the generation of hydroxyl radicals (both favoured under alkaline conditions), but rather the direct reaction between ozone and CBZ, which is swift enough to cause its complete elimination in a very short time. After the first 10 min, CBZ concentrations remain below

detection limits, confirming the effectiveness of the process and indicating that the influence of pH is mainly manifested in later stages, associated with the degradation of intermediates and partial mineralisation of the system.

The rapid elimination of CBZ under all tested conditions demonstrates the potential of ozonation as a robust tool for sustainable removal of recalcitrant pharmaceutical pollutants in advanced water treatment systems.

3.2. pH Kinetics During CBZ Ozonation

During the ozonation of CBZ in aqueous solution, the pH of the medium undergoes significant variations that reflect the chemical evolution of the system and the progressive transformation of organic matter (see Figure 3). It is important to emphasise that the experiments conducted at very high pH values (≥12) were not intended to represent operational conditions for full-scale wastewater treatment plants. Instead, these tests were specifically designed to isolate and elucidate the mechanistic influence of alkalinity on ozone decomposition, mass transfer behaviour, and the transition from molecular-ozone to radical-driven oxidation pathways. Such extreme pH conditions enable a clearer interpretation of reaction regimes that would be more difficult to distinguish in real wastewater matrices, where buffering capacity and typical operational constraints prevent large pH adjustments. Therefore, the high-pH results presented in this study should be understood as mechanistic benchmarks rather than practical recommendations for full-scale ozonation processes.

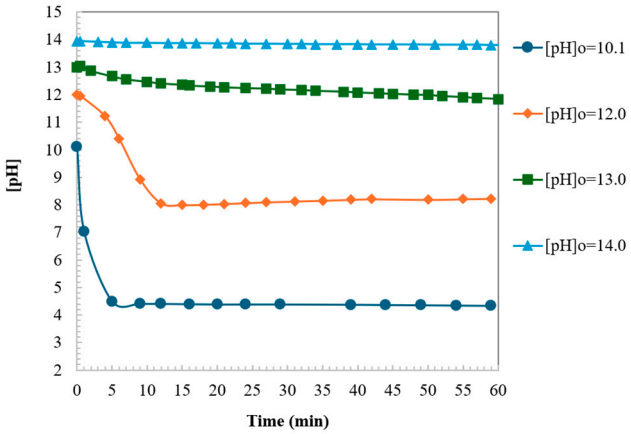


Figure 3. pH kinetics during CBZ ozonation. Experimental conditions: $[CBZ]_0$ = 50.0 mg/L; [T] = 25 °C; $[O_3]_{gas}$ = 58.5 g/Nm^3.

Although real wastewater typically presents pH values between 6 and 8, the pH 10–14 used in this study corresponds to initial pH conditions, selected exclusively to isolate the mechanistic influence of alkalinity on ozone decomposition and the transition between molecular-ozone and radical-dominated oxidation pathways. These conditions are not intended to represent full-scale operational pH but to function as a mechanistic probe. Importantly, the system does not maintain such alkaline values during ozonation. The experimental results show that the pH evolves rapidly within the first minutes of reaction: an initial pH of 10 decreases sharply to ≈4 within 5 min; an initial pH of 12 decreases and stabilises around ≈8; an initial pH of 13 drops slightly and stabilises near ≈12; and an initial pH of 14 remains essentially unchanged. Thus, even when the process begins at highly alkaline pH, the operative pH conditions during ozonation can shift toward neutral or even acidic environments depending on the initial alkalinity and the accumulation of acidic intermediates.

The recorded kinetics show that four different initial pH values were evaluated; however, in all cases, the pH changes significantly during the first few minutes of reaction.

Equation (1) shows the pH values measured after 2 h of the ozonation treatment as a function of the initial pH values of the water. Equation (1) was derived from an empirical linear fit of the experimental pH values measured after 2 h of ozonation. Its purpose is solely to describe the trend observed under the specific conditions of this study, and it is not intended as a mechanistic model or a generally applicable relationship. This simplification provides a practical way to visualise how the final pH responds to the initial alkalinity, but its validity is limited to the controlled experimental framework used here.

$$[\mathrm{pH}] = 2.4901[\mathrm{pH}]_0 - 21.013\mathrm{R}^2 = 0.9869 \quad (1)$$

This behaviour is mainly attributed to the formation of oxygenated intermediate species, many of which are acidic in nature. These products include aldehydes, ketones and, especially, low molecular weight carboxylic acids, whose transient accumulation leads to an initial acidification of the medium before the acid-base equilibrium conditions specific to each system are established.

In the experiment initiated at pH 10.1, a pronounced decrease in pH was observed, reaching approximately 4.0 within the first five minutes of ozonation. Thereafter, the pH remains virtually constant for the rest of the experiment. This rapid acidification indicates that, although the test starts under alkaline conditions, the oxidation of CBZ takes place mainly in an acidic environment. This shift has direct implications for the predominant reaction pathways and the reactivity of molecular ozone toward the various intermediates formed.

Several studies have thoroughly identified the intermediates formed during CBZ ozonation, providing strong experimental evidence of the reaction pathways affected by the pH-dependent shift between molecular ozone and hydroxyl radical oxidation. Among the most frequently reported intermediates are hydroxylated derivatives such as hydroxy carbamazepine and epoxy carbamazepine, along with more conjugated species including 1 (2 benzaldehyde)-4-hydro-(1H,3H)-quinazoline 2 one (BQM) and 1 (2 benzaldehyde)-(1H,3H)-quinazoline 2,4 dione (BQD), which are consistently observed as primary aromatic by-products. Experimental studies using HPLC-DAD, LC-MS and HRMS have confirmed the formation of these intermediates and demonstrated that, while CBZ is fully degraded within minutes, BQM and BQD exhibit higher persistence and slower oxidation, especially under conditions dominated by molecular ozone. Additional experimental evidence shows the formation of aldehydes, carboxylic acids and short-chain oxidation products that accumulate particularly at low and moderate alkalinity, correlating with the strong pH drop observed at pH $\approx$ 10.1 as acidic intermediates transiently accumulate. These findings support that the shift in oxidative regime directly determines the dominant intermediates, their transformation rates, and their stability during ozonation [25,26].

In contrast, when ozonation is initiated at pH 12.0, the decrease in pH is more moderate and stabilises around 8.0 after ten minutes, remaining practically constant thereafter. This stabilisation suggests that, once this value is reached, the system is buffered by the equilibrium of dissolved inorganic carbon in its various forms, mainly H_2CO_3 and HCO_3^-, which act as pH regulators in mildly alkaline media [28,29]. This buffering behaviour is consistent with the well established carbonate system equilibria operating in natural and laboratory aqueous media [29]. Carbon dioxide produced during the oxidation of organic matter rapidly hydrates to form carbonic acid (H_2CO_3), which partially dissociates into bicarbonate (HCO_3^-), thereby generating the conjugate acid–base pair responsible for pH regulation. The presence and coexistence of these species in water are widely documented through acid–base equilibrium measurements, spectrophotometric determinations and classic carbonate system speciation studies, which confirm the reactions $CO_2(aq) + H_2O \rightleftharpoons H_2CO_3$ and $H_2CO_3 \rightleftharpoons H^+ + HCO_3^-$. These equilibria have been

extensively validated in controlled aqueous systems and underpin the buffering capacity attributed to dissolved inorganic carbon (DIC) in mildly alkaline media.

Under stronger alkaline conditions (initial pH values of 13.0 and 14.0), the behaviour of the system differs significantly from the previous cases. When ozonation starts at pH 13.0, only a slight decrease in pH is observed, with values remaining close to 12 even after 60 min of reaction. This stability can be attributed to the high initial alkalinity of the medium, which effectively buffers any contribution of acidic species generated during the degradation of CBZ. Furthermore, the test that started at pH 14.0 shows no remarkable pH variations throughout the kinetics, confirming the robustness of the system against the incorporation of acidic oxidation products. In this pH range, the buffering capacity is high enough to completely suppress the acidification observed under moderately alkaline conditions.

The use of extremely alkaline conditions (pH 14) in this study does not aim to replicate operational conditions in real water-treatment systems. Instead, pH 14 was selected as an initial mechanistic benchmark to isolate the radical-dominated oxidation regime resulting from the near-instantaneous decomposition of ozone at very high alkalinity. Importantly, these values represent initial conditions only; experimental data show that the pH rapidly shifts during ozonation, with pH_0 = 10 dropping to ≈4, pH_0 = 12 decreasing to ≈8, pH_0 = 13 stabilising near ≈12, and pH_0 = 14 remaining unchanged. Using such extreme initial alkalinity enables the clear differentiation between molecular-ozone and radical pathways, a distinction that is obscured at neutral pH due to buffering capacity and radical scavenging in real wastewater matrices. Therefore, pH 14 provides essential mechanistic insight relevant to advanced oxidation processes, particularly those designed to enhance ozone decomposition and hydroxyl radical formation, even though it is not proposed for practical full-scale operation.

It is also relevant to note that the pH evolution observed, particularly the pronounced acidification at an initial pH of 10.1, is not solely governed by the transient formation of early oxygenated intermediates, but by the subsequent accumulation of low-molecular-weight carboxylic acids generated during the deeper oxidation stages of CBZ. While the first aromatic and heterocyclic intermediates are rapidly transformed, their further degradation produces short-chain mono- and dicarboxylic acids that persist within the experimental timeframe and therefore prevent any return to the initial pH. Under strongly alkaline conditions ($pH_0 \geq 13$), these acidic species remain largely deprotonated due to the high buffering capacity of the carbonate/bicarbonate system, which suppresses measurable pH decline despite their formation. Thus, the final pH reached in each experiment reflects the balance between the rate of acidic intermediate production, their incomplete mineralisation, and the inherent alkalinity of the medium. This behaviour is consistent with the well-documented ozonation pathways of recalcitrant aromatic pollutants and explains why pH stabilises at values lower than the initial ones even after complete CBZ depletion.

Therefore, the evolution of pH during CBZ ozonation results from the combination of two main processes: the rapid generation of acidic intermediate products during the early stages of degradation and their following mineralisation into carbon dioxide. The released CO_2 equilibrates with water to form carbonic acid and, subsequently, bicarbonate and carbonate species depending on the pH. In this way, the system tends to stabilise at a pH value determined by the equilibrium of the $CO_2/H_2CO_3/HCO_3^-$ pair and by the total alkalinity available in the solution. In media with low initial alkalinity, such as those starting at pH 10.1, the accumulation of acid intermediates dominates the behaviour and leads to acidic conditions. In contrast, in more alkaline media, such as tests started at pH 12.0–14.0, the buffering capacity associated with the carbonate-bicarbonate system together with the high concentration of strong bases moderates acidification and promotes pH stabilisation at neutral or alkaline values.

The pH evolution in each case determines the chemical regime under which ozonation occurs. In acidic environments, the direct reaction of molecular ozone predominates due to its greater stability and lower tendency to decompose into radical species. As the medium becomes more alkaline, ozone decomposition and formation of hydroxyl radicals ($OH^{\bullet}$) are enhanced, introducing a less selective and more reactive oxidative pathway towards a wide range of organic compounds. Thus, the differences observed between the kinetics developed under different initial pH values should not be interpreted solely in terms of the starting pH value, but rather by considering the pH trajectory throughout the reaction and the effective time during which the system remains within each pH range.

Overall, the common pattern observed in all tests—an initial drop in pH followed by a stabilisation stage—serves as an indirect indicator of the sequence of processes that take place during ozonation: formation of acidic intermediates, their transformation and subsequent mineralisation, and the final establishment of an equilibrium guided by the species in the carbonic system. The evolution of pH provides valuable insight into the oxidation mechanisms, the buffering capacity of the medium, and the state of progress of organic mineralisation. Therefore, its interpretation must be systematically integrated into the discussion of the kinetic and mechanistic results associated with the degradation of CBZ by ozone.

3.3. Loss of Water Aromaticity

During CBZ ozonation, the loss of aromaticity in water is a key indicator of the compound's degradation degree. Figure 4 shows the evolution of water aromaticity during CBZ ozonation. Aromaticity refers to the presence of conjugated aromatic structures in the dissolved organic matter and oxidation intermediates. In this study, aromaticity was quantified by measuring the UV absorbance at 254 nm, a wavelength commonly associated with π–π transitions in aromatic rings. A decrease in A_{254} indicates progressive disruption of aromatic structures during CBZ oxidation. Although the transient increase in aromaticity is consistent with the formation of oxygenated aromatic intermediates commonly reported during CBZ ozonation, these species were not experimentally identified in the present study. Therefore, the interpretation provided is based solely on indirect evidence—namely, the temporal evolution of UV absorbance, colour development, and literature reports.

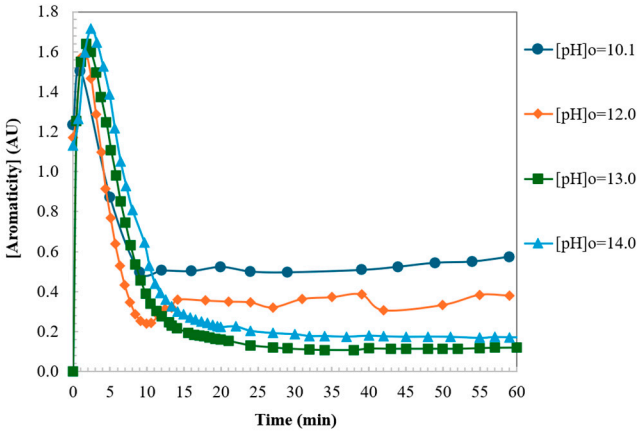


Figure 4. Aromaticity changes during CBZ ozonation. Experimental conditions: $[CBZ]_0$ = 50.0 mg/L; [T] = 25 °C; $[O_3]_{gas}$ = 58.5 g/Nm^3.

As observed, aromaticity increases during the first 3 min of the reaction until it reaches a maximum value, whose magnitude clearly depends on the operating pH. The greatest increase in aromaticity is observed at pH = 14.0, indicating that strongly alkaline conditions favour the initial formation of oxygenated aromatic intermediates with conjugated systems

capable of absorbing in the UV region. After reaching this maximum, the aromaticity progressively decreases, reflecting the degradation of these intermediates into less conjugated or totally aliphatic compounds. The level of residual aromaticity remaining in the treated water also depends on the initial pH. Operating at pH = 13.0 leads to the greatest overall reduction in aromaticity, evidencing a more extensive degradation of the aromatic intermediate compounds under these conditions. In contrast, when the treatment is carried out at pH = 10.1, the highest residual aromaticity is obtained, suggesting that the breakdown of aromatic systems is less efficient and that more refractory structures (less susceptible to oxidation) persist in the medium.

These results confirm that both the formation and removal of aromatic intermediates are strongly pH-dependent processes: (i) Highly alkaline pH (≈14.0): Promotes the rapid formation of chromophores, although these compounds are also subsequently degraded; (ii) Moderately high alkaline pH (≈13.0): Provides the most favourable balance between initial formation and deep oxidation, resulting in the greatest net reduction in aromaticity; (iii) Moderately alkaline pH (≈10.0–12.0): Limits the overall oxidative capacity of the system, allowing the accumulation of refractory aromatic residues in the treated water.

The progressive decrease in absorbance within the characteristic spectral region of aromatic rings reflects the breakdown of the CBZ molecular structure. This behaviour is attributed to the high reactivity of ozone, which preferentially attacks the conjugated double bonds present in the aromatic nucleus, initiating addition and oxidation reactions that lead to ring opening. As ozonation progresses, aromaticity decreases significantly, indicating the formation of less complex intermediate products, such as aliphatic compounds and carboxylic acids.

The use of a micro-diffuser that generates microbubbles substantially enhances the mass transfer of ozone. Microbubbles provide a larger interfacial surface area and exhibit longer residence times in the liquid phase, which increases the solubilisation of ozone and promotes its decomposition into hydroxyl radicals. These highly reactive radical species accelerate the breakdown of the conjugated double bonds present in aromatic rings. Consequently, the loss of aromaticity is faster and more complete, indicating more efficient CBZ degradation and increased formation of oxygenated intermediate products.

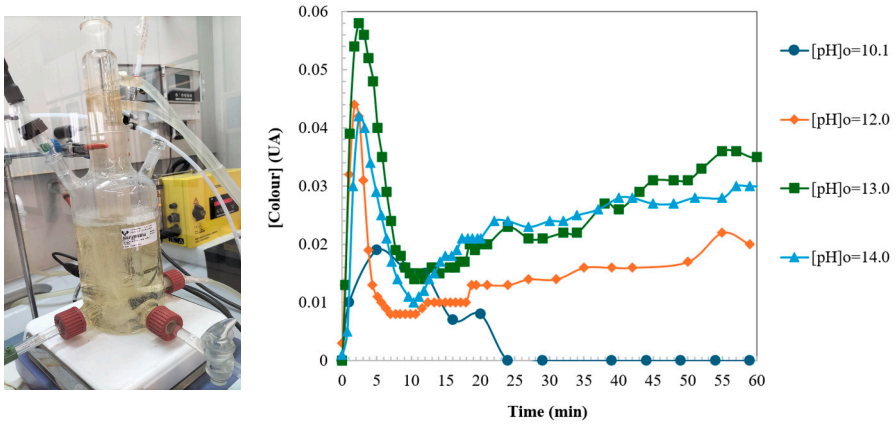
This phenomenon is closely related to the partial mineralisation of the contaminant. However, the complete disappearance of aromaticity does not necessarily imply the total elimination of organic carbon, as oxygenated fragments may persist in solution. This observation is particularly relevant, as the loss of aromaticity is considered a critical step towards water detoxification and reducing the persistence of the contaminant.

3.4. Chromatic Changes in Ozonated Water

The initial aqueous solution of CBZ is colourless. However, the injection of ozone in the form of microbubbles increases ozone solubilisation and prolongs the gas–liquid contact time, promoting the degradation of CBZ through oxidative pathways that lead to the formation of coloured intermediate compounds [23]. The maximum colour intensity is reached approximately 3 min after the start of the ozonation, resulting in a bright yellow aqueous solution as seen in Figure 5a.

The yellow colour is attributed to the generation of oxygenated aromatic intermediates with conjugated systems capable of absorbing in the visible region. Among the main intermediates identified during CBZ degradation by ozone and hydroxyl radicals are: 1-(2-benzaldehyde)-4-hydroxy-1H-benzotriazole (BQM), 1-(2-benzaldehyde)-1H-benzotriazole (BZD), 1-(2-carboxaldehyde)-1H-benzotriazole (BZO), acridone and oxygenated acridine derivatives, hydroxy-CBZ and epoxy-CBZ derivatives (particularly CBZ-10,11-epoxide, which can further evolve into more highly conjugated products). These

intermediates have partially open or oxygenated aromatic rings, with functional groups such as aldehydes or conjugated heterocyclic systems responsible for the yellowish colour observed. The degradation intermediates were not directly detected or quantified. Therefore, the intermediates mentioned are inferred from well established pathways reported in the literature, while in this study their presence is supported only indirectly through the observed evolution of colour, aromaticity, turbidity and ozone stability.



(**a**) (**b**)

Figure 5. (**a**) Yellow colour generated in water. Experimental conditions: $[CBZ]_0$ = 50.0 mg/L; $[pH]_0$ = 14.0; [T] = 25 °C; $[O_3]_{gas}$ = 58.5 g/Nm^3 (**b**) Variation in water colour during CBZ ozonation. Experimental conditions: $[CBZ]_0$ = 50.0 mg/L; [T] = 25 °C; $[O_3]_{gas}$ = 58.5 g/Nm^3.

Once the maximum formation of coloured intermediates is reached, the generation of hydroxyl radicals in the presence of microbubbles promotes the progressive degradation of these compounds. This behaviour is attributed to the breakdown of the conjugated systems responsible for absorption in the visible spectrum, leading to a gradual decrease in colour intensity. This phenomenon is associated with the structural disruption of aromatic rings and the formation of more oxygenated products with fewer chromophore groups, such as short-chain carboxylic acids. Therefore, colour disappearance is an indirect indicator of the elimination of aromatic and chromophore structures formed during CBZ degradation.

Figure 5b shows the variation in water colour during the ozonation of CBZ at different pH values under a high ozone dose (58.5 g/Nm^3). The observed behaviour is characterised by an initial increase in colour intensity, followed by a gradual decrease until the treated water becomes colourless. This phenomenon is attributed to the transient formation of chromophore intermediate products and the influence of pH on the rate of oxidation reactions.

When operating at pH 10.1, ozone decomposition proceeds slowly and direct oxidation of CBZ predominates. This condition favours the accumulation of chromophore intermediates, which explains the longer persistence of the initial peak of colour before its subsequent elimination. Under stronger alkaline conditions, the results indicate the occurrence of two stages in colour formation associated with the CBZ degradation pathway leading to the formation of coloured species.

The first stage (0–10 min) of the CBZ decomposition leads to the formation of highly coloured intermediates. This stage involves hydroxylation reactions resulting from the electrophilic attack of hydroxyl radicals on the olefinic double bond located within the central and lateral heterocyclic rings of the CBZ molecule, leading to the formation of the corresponding hydroxylated CBZ derivatives. The action of hydroxyl radicals can generate further hydroxylation, leading to the creation of cis- and trans-dihydroxycarbamazepine. The formation of the cis isomer has been reported to occur to a lesser extent than that of

the trans isomer. Subsequent oxidation of these species leads to the formation of coloured precursors, oxo- and dioxo-carbazepines (10-OH-CBZ, 9-OH-CBZ, EP-CBZ, OX-CBZ), whose molecular structures contain chromophore groups responsible for their colour.

During the second stage of colour formation (10–60 min), additional species are generated that coexist with those formed in the previous stage, although they contribute less to colour intensity to the water. In this phase, the formation of secondary degradation by-products of carbamazepine species can be considered, including hydroxylated acridine molecules (9-OH-acridine) and their corresponding acridones that contribute to the residual colour observed.

Finally, ozonation treatment under the conditions tested is capable of progressively mineralising these degradation intermediates (leading to the formation of carbon dioxide, ammonium and nitrates) until colourless treated water is obtained.

3.5. Turbidity Development in Water

Figure 6 illustrates the variation in water turbidity during CBZ ozonation at different pH values, using a high ozone dose (58.5 g/Nm^3). A clear pH-dependent behaviour is observed, characterised by increases in turbidity whose magnitude, kinetics and persistence differ significantly depending on the basicity of the medium [6].

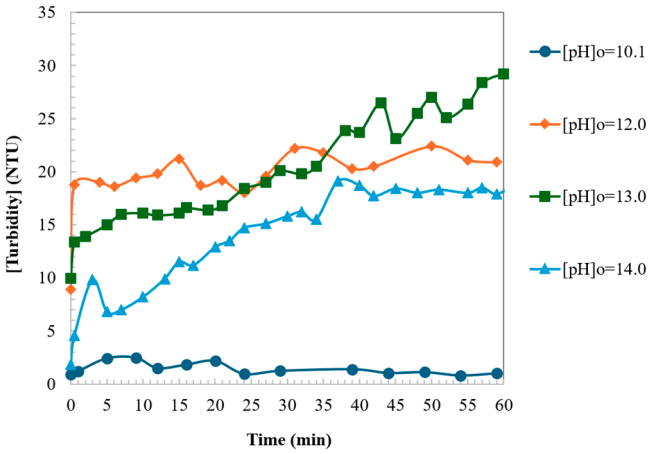


Figure 6. Variation in water turbidity during CBZ ozonation. Experimental conditions: $[CBZ]_0$ = 50.0 mg/L; [T] = 25 °C; $[O_3]_{gas}$ = 58.5 g/Nm^3.

At pH 10.1, ozone decomposition is relatively slow, with direct oxidation by molecular ozone predominating over radical pathways. Under these conditions, the formation or degradation of intermediates occurs gradually and no significant colloidal particles or aggregates are generated. Consequently, turbidity remains nearly constant throughout the process (remaining below 2.5 NTU). According to World Health Organization (WHO) guidelines, drinking water should not exceed 5.0 NTU, and values below 1 NTU are generally recommended under standard treatment conditions.

When the pH rises to 12.0, the rate of ozone decomposition is significantly enhanced, leading to a higher concentration of hydroxyl radicals. This increase in radical activity accelerates the CBZ oxidation, promoting the temporary formation of partially oxidised products capable of destabilising the aqueous matrix and generating fine particles or colloidal aggregates. As a result, turbidity reaches significantly higher values, approaching 20.0 NTU, reflecting a greater presence of dispersed species in the medium. The marked increase in turbidity observed under strongly alkaline conditions was interpreted as the possible formation of transient colloidal or aggregated species; however, these particles were not characterised experimentally in this study. This interpretation is therefore based solely on indirect evidence.

Under strongly alkaline conditions, such as pH 13.0 and 14.0, ozone decomposition is extremely rapid, producing very high concentrations of hydroxyl radicals. This high reactivity induces intense and accelerated oxidation, simultaneously generating large amounts of intermediates and transient by-products that increase turbidity throughout the process. In this pH range, turbidity exhibits an almost linear increase throughout the treatment, indicating continuous formation of particles or aggregates. In particular, at pH = 13.0, the most pronounced turbidity increase is observed, reaching values close to 30.0 NTU after 60 min of reaction.

Overall, the results presented in Figure 6 demonstrate that pH acts as a key regulator of the balance between direct and radical oxidation mechanisms, determining the nature, quantity and accumulation of the formed intermediates. As the pH increases, the reaction progressively shifts towards radical pathways, promoting the formation of transient particulate species and, as a result, higher turbidity values during ozonation. Several experimental indicators (ozone stability, mass-transfer behaviour, turbidity formation, and colour dynamics) confirm the progressive shift of the oxidation mechanism towards radical pathways, even though direct radical detection was not performed in this study. It is important to highlight that the water treated in this study is not intended for direct consumption. Turbidity values reported here reflect the mechanistic response of ozonation under controlled conditions; in practical applications, further treatment stages would be required to reduce turbidity and ensure compliance with drinking-water or discharge standards.

These water-quality indicators are particularly relevant from a sustainability standpoint, as colour and turbidity directly affect the acceptability and reuse potential of treated effluents, highlighting the importance of controlling oxidation conditions beyond contaminant removal alone.

3.6. Ozone Gas Concentration During the Ozonation Process

Figure 7 illustrates the evolution of the ozone gas concentration in the reactor ($[O_3]_{gas}$, g/Nm^3) as a function of the initial pH of the treated water. The data are plotted in a normalised form with respect to the initial ozone concentration fed to the reactor ($[O_3]_{gas,0}$, g/Nm^3). As observed, the gas-phase ozone concentration decreases sharply during the first 2 min of reaction, reaching a characteristic minimum value in this initial stage. This initial drop is due to the high oxidising demand of the medium, in which both CBZ and the first intermediates rapidly react with the ozone transferred from the gas to the liquid phase.

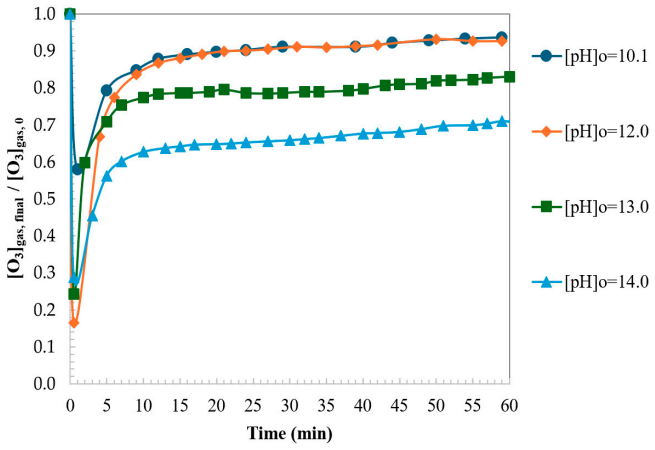


Figure 7. Variation in ozone gas concentration in the reactor during CBZ ozonation. Experimental conditions: $[CBZ]_0$ = 50.0 mg/L; [T] = 25 °C; $[O_3]_{gas}$ = 58.5 g/Nm^3.

Subsequently, the ozone gas concentration progressively increases as CBZ degrades and the ozone consumption capacity of the medium diminishes. This increase continues until stable values ($[O_3]_{gas,final}$, g/m^3) are reached. These final concentrations depend on the initial pH of the treated water, as shown in Equation (2), indicating that an equilibrium is established between gas–liquid transfer and oxidant consumption.

$$\frac{[O_3]_{gas,final}}{[O_3]_{gas,0}} = -0.0274[pH]_0^2 + 0.6032[pH]_0 - 2.3773 \quad (2)$$

The results show that alkaline pH values lead to higher final gas-phase ozone concentrations. This behaviour is consistent with ozone chemistry in aqueous systems: at alkaline pH, ozone decomposition increases through hydroxyl radical formation, while the direct reaction rate of molecular ozone with some aromatic compounds such as CBZ decreases. As a result, the competition between radical-driven pathways and direct ozone consumption alters the overall oxidant demand of the medium, allowing ozone to accumulate more rapidly in the system once most of the contaminant has been degraded.

Overall, the system operates under two distinct regimes: (i) initial high demand regime, where the transferred ozone is rapidly consumed, causing a sharp decrease in gas-phase ozone concentration; (ii) saturation or quasi-equilibrium regime, where the oxidant demand of the environment is substantially reduced and ozone begins to accumulate in both the gas and liquid phases, eventually stabilising at values close to the feed concentration.

3.7. Ozone Dissolved in Water

Figure 8 shows the evolution of dissolved ozone concentration in water during the CBZ ozonation process. Analysis of these curves reveals three fundamentally distinct patterns that describe the change in the chemical regime experienced by the system as alkalinity increases: a regime of moderate accumulation at initial pH 10.1; a regime of accelerated decomposition at pH 12.0–13.0; and an extreme regime at pH 14.0, where the concentration of dissolved ozone is practically residual.

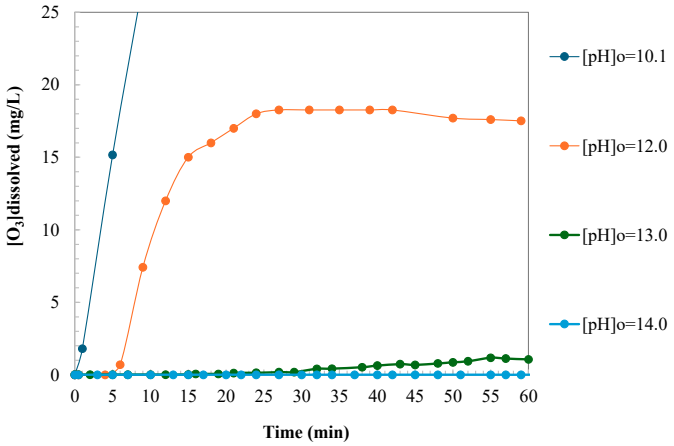


Figure 8. Variation in ozone gas concentration dissolved in water during CBZ ozonation. Experimental conditions: $[CBZ]_0$ = 50.0 mg/L; [T] = 25 °C; $[O_3]_{gas}$ = 58.5 g/Nm^3.

The results demonstrate a strong dependence of ozone stability on pH, reflecting a progressive change in the oxidative regime from molecular to radical pathways as alkalinity increases. At initial pH 10.1, dissolved ozone reaches relatively high values, indicating that the gas–liquid transfer rate exceeds the rate of oxidant decomposition. It is important to clarify that dissolved ozone does not remain at a fixed solubility limit during semi-continuous ozonation. In our system, ozone was injected continuously at a high gas-phase

concentration and with microbubble diffusers, which significantly enhance gas–liquid mass transfer. Under these conditions, dissolved ozone progressively accumulates in the liquid phase as the oxidation of CBZ proceeds and the ozone demand of the medium decreases.

At initial pH 12.0 and 13.0, the steady-state ozone concentration decreases significantly (≈2 and 17.0 mg/L), and stabilisation occurs earlier. This decrease reflects the acceleration of ozone decomposition by OH^- attack, which promotes the formation of hydroxyl radicals and reduces the accumulation of molecular ozone in solution.

The most extreme behaviour is observed at pH 14.0, where dissolved ozone remains close to residual values throughout the process. The extremely high concentration of OH^- under these conditions leads to an almost instantaneous decomposition of the oxidant, preventing its accumulation, thus establishing a regime dominated by short-lived radical species.

Overall, the results indicate that the stability of ozone in the aqueous phase decreases sharply with pH, controlling the transition from an oxidative mechanism dominated by molecular ozone (pH 10.1) to an intensive radical mechanism (pH $\geq$ 12). This transition determines the nature of the predominant oxidants and, therefore, the selectivity and efficiency of the ozonation process.

3.8. Estimation of the Volumetric Mass Transfer Coefficient of Ozone

The estimation of the volumetric mass transfer coefficient of ozone (k_{La}) under different initial pH conditions was carried out using the classical dynamic method for gas–liquid systems, which has been successfully applied to assess the combined effect of pH and mass transfer during ozonation of pharmaceutical contaminants [30]. This approach relies on monitoring the temporal evolution of the dissolved ozone concentration in a well-mixed batch reactor subjected to a constant gas-phase ozone concentration. The dynamic mass balance for ozone in the liquid phase assumes that no chemical reaction takes place initially or, alternatively, that any reaction can be incorporated into an "apparent" mass transfer coefficient when the oxidant undergoes rapid consumption. Under these conditions, the transient mass balance for ozone in the liquid phase is expressed as (Equation (3)):

$$\frac{dC(t)}{dt} = k_{La}(C^* - C(t)) \quad (3)$$

where

C(t): dissolved ozone concentration at time t (mg/L)
C*: equilibrium concentration of ozone in water (gas–liquid saturation concentration) (mg/L)
k_{La}: volumetric mass transfer coefficient to be determined (1/min)

Assuming constant hydrodynamics and gas-phase conditions, the differential equation can be integrated analytically, yielding (Equation (4)):

$$C(t) = C^*[1 - \exp(-k_{La}t)] \quad (4)$$

which can be rearranged into the linearized form (Equation (5)):

$$\ln(C^* - C(t)) = -k_{La}t + b \quad (5)$$

where (Equation (6))

$$b = \ln(C^*) \quad (6)$$

This linear form enables the estimation of k_{La} through a linear regression of $\ln(C^* - C(t))$ versus time. Only experimental points corresponding to the ozone accu-

mulation phase—i.e., before approaching saturation—were used in the regression to avoid distortions associated with noise near the plateau region.

In cases where the initial pH was sufficiently high (pH $\geq$ 12), the rapid decomposition of ozone in an alkaline medium results in a strong deviation from ideal dynamic behavior. Under these conditions, the dissolved concentration remained close to zero during most of the experiment, even though gas-phase ozone was continuously supplied. In such scenarios, the model above does not describe pure mass transfer but instead describes an apparent dynamic process governed by both transfer and rapid chemical consumption. Consequently, the estimated parameter corresponds to an apparent k_{La}, denoted as in Equation (7):

$$k_{La,app} = k_{La} + k_{reaction} \quad (7)$$

where $k_{reaction}$ (1/min) represents the first-order contribution of the ozone decomposition rate in a strongly alkaline medium. As pH increases, $k_{reaction}$ increases exponentially due to the well-known dependence of ozone decomposition on hydroxide ion concentration, leading to progressively larger deviations between the theoretical and the experimental dynamic profiles.

At extremely alkaline pH (pH 14), the decomposition of ozone is essentially instantaneous. In this condition, dissolved ozone remains negligible throughout the experiment (Equation (8)):

$$C(t) \approx 0 \quad (8)$$

which prevents the application of the dynamic model, as the logarithmic term in the linearization becomes constant (Equation (9)):

$$\ln(C^* - C(t)) \approx \ln(C^*) \quad (9)$$

and the slope of the regression tends to zero, yielding (Equation (10)):

$$k_{La,app} \approx 0 \quad (10)$$

This value does not correspond to a physical mass transfer limitation but instead reflects the impossibility of measuring transfer under conditions where ozone reacts faster than it can accumulate in the liquid phase. Overall, the mathematical model used enables reliable estimation of k_{La} at pH values where ozone remains sufficiently stable to accumulate measurably in the aqueous phase. At higher pH values, the results must be interpreted as apparent mass transfer coefficients, where chemical instability of ozone dominates the observed dynamics. Figure 9 presents a schematic representation of the proposed model for estimating the ozone mass transfer coefficient (k_{La}). Based on the proposed mathematical model, the volumetric ozone mass transfer coefficients were estimated as a function of the initial pH of the aqueous carbamazepine solution. The resulting values are presented in Table 1.

Table 1. Volumetric mass transfer coefficients of ozone estimated using the proposed mathematical model.

$[pH]_0$	C* (mg/L)	k_{La} (1/min)
10.1	54.8	0.0807
12.0	18.26	0.1760
13.0	1.17	0.0427
14.0	0	0

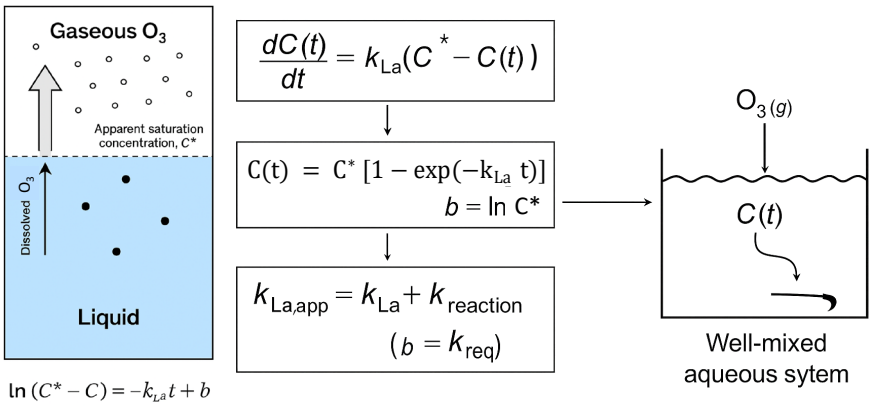


Figure 9. Scheme of the mathematical modelling used to estimate the volumetric mass transfer coefficient of ozone.

The evolution of the volumetric mass transfer coefficient for ozone (k_{La}) shows a marked dependence on the initial pH of the aqueous solution, reflecting the interaction between gas–liquid transfer processes and the chemical stability of the oxidant in water. At moderately basic conditions ($[pH]_0 \approx 10.1$), ozone remains sufficiently stable to allow its progressive accumulation in the liquid phase, giving rise to the characteristic increase in dissolved O_3 concentration. Under these conditions, mass transfer governs the behavior of the system, and a k_{La} value of 0.0807 1/min is obtained, which is fully consistent with expectations for a fine-bubble diffuser operating at low gas flow rates and with moderate dispersion efficiency.

When the pH is increased to values around $[pH]_0$ 12, a notable rise in the apparent k_{La} (0.176 1/min) is observed. This increase should not be interpreted as a genuine improvement in the intrinsic transfer efficiency of the system, but rather as a direct consequence of the rapid consumption of ozone in the liquid phase due to its accelerated decomposition under strongly alkaline conditions. At this pH, the reaction between O_3 and OH^- produces radicals and intermediate species that reduce the dissolved ozone concentration almost immediately, keeping it far below its equilibrium value (C*). This results in a persistently high gas–liquid concentration gradient throughout the experiment ($C^* - C \approx C^*$), which mathematically manifests as an elevated apparent k_{La}. Consequently, the value obtained reflects both the transfer process and the strong chemical demand of the oxidant.

As the initial pH increases further to values close to 13, the stability of ozone is even more severely compromised and the oxidant is destroyed almost instantaneously. Under these conditions, the concentration of dissolved O_3 remains near zero for nearly the entire experimental period, which drastically reduces the quality of the dynamic adjustment and leads to a much lower apparent k_{La} value (0.0427 1/min). In this scenario, the decomposition kinetics completely dominate over gas–liquid transfer, and the absence of measurable ozone accumulation in the liquid phase makes it impossible to obtain a representative value of the actual mass transfer coefficient.

Finally, at $[pH]_0$ 14 the decomposition of ozone is virtually instantaneous, and no detectable accumulation of dissolved O_3 is recorded at any point during the experiment. As a result, the dynamic method cannot be applied and the mathematical adjustment yields k_{La} = 0 1/min. This outcome does not indicate a true absence of mass transfer, but rather the impossibility of measuring it due to the immediate destruction of the oxidant in an extremely alkaline environment. Under these conditions, all transferred ozone reacts instantaneously, eliminating any possibility of observing an accumulation phase.

Overall, the results demonstrate that the k_{La} obtained from dynamic experiments is representative of the gas–liquid transfer process only when ozone exhibits sufficient stability

in the aqueous phase. At high pH, the values are strongly influenced by decomposition kinetics and must therefore be regarded as "apparent coefficients", in which the effects of pH and system reactivity outweigh the intrinsic mass transfer mechanism.

Understanding the interplay between ozone stability and apparent mass-transfer behaviour is therefore essential for the sustainable design and optimisation of ozonation-based advanced oxidation processes.

4. Discussion

The results clearly demonstrate that ozonation is a highly effective treatment for the rapid degradation of carbamazepine (CBZ), achieving complete removal within the first 10 min, regardless of the initial pH. This confirms that the early stage of the process is dominated by the high availability of molecular ozone, which reacts rapidly with CBZ before pH-dependent radical pathways become predominant. Once most of the parent compound is degraded, however, the evolution of the system becomes strongly governed by pH, influencing both the reaction mechanisms and the behaviour of transformation products.

At pH 10.1, the marked drop to pH $\approx$ 4.0 within 5 min indicates the accumulation of acidic oxygenated intermediates. In contrast, at pH 13.0–14.0, the pH remains stable, reflecting the strong buffering capacity of highly alkaline media and the rapid decomposition of ozone into hydroxyl radicals. This shift in oxidative regime is consistent with the measured ozone profiles: dissolved ozone reaches >20.0 mg/L at pH 10.1, whereas at pH 14 it remains nearly zero due to instantaneous decomposition, and gas-phase ozone exhibits the characteristic initial decline followed by pH-dependent recovery. These trends collectively confirm a transition from a molecular-ozone-dominated regime at lower alkalinity to a radical-dominated regime under highly alkaline conditions. Although direct radical detection was not performed, several experimental indicators obtained in this study—including dissolved ozone stability, mass transfer behaviour, turbidity formation, and colour dynamics—are consistent with the well-established transition from molecular ozone oxidation to radical pathways at high pH.

The behaviour of aromaticity, colour, and turbidity further supports this mechanistic interpretation. The appearance of a pronounced yellow coloration within the first 3 min, particularly at pH 14.0, indicates the rapid formation of conjugated aromatic intermediates. Their subsequent decline reflects continued oxidation and ring-opening reactions. Turbidity trends also show clear pH dependence: values remain below 2.5 NTU at pH 10.1, suggesting limited formation of particulate by-products, while turbidity increases up to $\approx$30 NTU at pH 12.0–13.0, consistent with the generation of transiently dispersed species under radical-driven oxidation. These findings highlight that, although CBZ is removed quickly, the quality of the treated water can vary substantially depending on the pH, particularly regarding colour and particle formation.

From a broader perspective, these results align with previous studies reporting the persistence of CBZ in conventional treatments and the strong potential of ozone-based advanced oxidation processes to overcome its recalcitrance. The present work expands this understanding by demonstrating how the control of pH can shift oxidative pathways, influencing not only reaction kinetics but also the formation, stability, and removal of intermediates. This simplification enabled a clear mechanistic interpretation of the roles of pH, ozone stability and mass-transfer dynamics without the confounding effects introduced by ionic strength. Nevertheless, real water matrices typically contain significant concentrations of dissolved ions—such as chloride, sulfate, nitrate and bicarbonate—that can alter ozone solubility, shift the balance between molecular and radical oxidation pathways, and participate in scavenging or propagation reactions. These effects may influence both

the rate of CBZ degradation and the distribution of transformation products. While the present work sought to isolate fundamental behaviours under controlled conditions, future studies should evaluate the impact of ionic strength and common inorganic constituents to better replicate realistic water quality scenarios and strengthen the applicability of the mechanistic insights obtained here.

The experiments were performed using relatively high CBZ concentrations (50.0 mg/L) in simplified aqueous matrices, which may not fully represent the complexity of real wastewater containing natural organic matter or radical scavengers. It is also important to acknowledge that the experiments in this study were carried out using ideal aqueous solutions, intentionally free of inorganic salts or background electrolytes. This simplification enabled a clear mechanistic interpretation of the roles of pH, ozone stability and mass-transfer dynamics without the confounding effects introduced by ionic strength. Nevertheless, real water matrices typically contain significant concentrations of dissolved ions—such as chloride, sulfate, nitrate and bicarbonate—that can alter ozone solubility, shift the balance between molecular and radical oxidation pathways, and participate in scavenging or propagation reactions. These effects may influence both the rate of CBZ degradation and the distribution of transformation products. While the present work sought to isolate fundamental behaviours under controlled conditions, future studies should evaluate the impact of ionic strength and common inorganic constituents to better replicate realistic water quality scenarios and strengthen the applicability of the mechanistic insights obtained here.

Although the observed behaviour is consistent with the well-documented shift from molecular-ozone reactions to hydroxyl radical-dominated pathways at high pH, this transition was not experimentally verified in this study. The interpretation presented here is therefore based solely on indirect evidence—such as ozone stability, pH evolution, colour dynamics, and turbidity formation—and should be regarded as a plausible mechanistic explanation rather than a confirmed radical-mediated process. Direct detection or quantification of hydroxyl radicals and intermediate species was not carried out, but several experimental indicators obtained in this work—such as dissolved ozone decay, mass-transfer behaviour, turbidity formation, and colour dynamics—are consistent with the well-established transition from molecular ozone reactions to radical pathways at high pH. These interpretations are therefore based on indirect evidence and aligned with established literature, rather than on direct species identification. Additionally, while aromaticity, colour, and turbidity are useful indicators, comprehensive identification or quantification of by-products and mineralisation was not performed. Accordingly, the absence of TOC or COD measurements represents a limitation of this study, as mineralisation and total organic carbon removal could not be quantitatively assessed. These aspects merit further investigation to ensure safe and environmentally compatible treatment.

Future research should focus on evaluating ozonation under more realistic water matrices, performing detailed intermediate and toxicity analyses, and exploring hybrid treatment schemes that balance rapid CBZ degradation with improved control over colour and turbidity. Optimising mass transfer and operational pH—potentially through sequential or buffered stages—could further enhance process efficiency and water-quality outcomes.

From a sustainability perspective, the findings of this study underscore that effective removal of persistent pharmaceuticals such as carbamazepine is a key requirement for advancing sustainable water management strategies. While ozonation enables rapid contaminant degradation, the results demonstrate that operational parameters—particularly pH and mass transfer—must be carefully controlled to ensure not only chemical removal but also acceptable water-quality outcomes in terms of colour and turbidity. These insights

are directly relevant for the optimisation of advanced treatment stages aimed at wastewater reuse, environmental protection and the long-term sustainability of water resources.

Author Contributions: Conceptualization, N.V.; methodology, M.A.V.-C., U.D. and E.B.-G.; software, M.A.V.-C., E.B.-G., U.D. and N.V.; validation, M.A.V.-C., E.B.-G., U.D. and N.V.; formal analysis, M.A.V.-C., E.B.-G., U.D. and N.V.; investigation, M.A.V.-C., E.B.-G. and N.V.; resources, M.A.V.-C., E.B.-G. and N.V.; data curation, M.A.V.-C., E.B.-G., U.D. and N.V.; writing—original draft preparation, E.B.-G. and N.V.; writing—review and editing, N.V.; visualization, E.B.-G., U.D. and N.V.; supervision, N.V.; project administration, N.V.; funding acquisition, N.V. All authors have read and agreed to the published version of the manuscript.

Funding: This research was funded by PIBA_2023_01_0032—Basic and/or Applied Research Project. Financing entity: Basque Government 2023.

Institutional Review Board Statement: Not applicable.

Informed Consent Statement: Not applicable.

Data Availability Statement: The database is available upon request.

Acknowledgments: The authors thank the Department of Chemical and Environmental Engineering and the Department of Chemical Engineering of the University of the Basque Country UPV/EHU for their support.

Conflicts of Interest: The authors declare no conflicts of interest.

Abbreviations

The following abbreviations are used in this manuscript:

AOPs	Advanced Oxidation Processes
BQM	1-(2-benzaldehyde)-4-hydroxy-1H-benzotriazole
BZD	1-(2-benzaldehyde)-1H-benzotriazole
BZO	1-(2-carboxaldehyde)-1H-benzotriazole
CBZ	Carbamazepine
ECs	Emerging Contaminants
EC_{50}	Effective Concentration
EDCs	Endocrine-Disrupting Compounds
SDGs	Sustainable Development Goals
WHO	World Health Organization
WWTPs	Wastewater Treatment Plants

References

1. Lapworth, D.J.; Baran, N.; Stuart, M.E.; Ward, R.S. Emerging Organic Contaminants in Groundwater: A Review of Sources, Fate and Occurrence. *Environ. Pollut.* **2012**, *163*, 287–303. [CrossRef]
2. Verteegen, E.; Häkkinen, M.; Wu, D.; Heikamp-de Jong, I.; Roessink, I.; Peeters, E.T.H.M.; Van de Brink, P.J. Effects of the Drug Carbamazepine on the Structure and Functioning of a Freshwater Aquatic Ecosystem. *Ecotoxicol. Environ. Saf.* **2025**, *294*, 118009. [CrossRef]
3. Kumar, M.V. Advanced Oxidation Processes: An Effective Solution for Treating Emerging Pollutants from Pharmaceutical Industries. *E3S Web Conf.* **2024**, *596*, 01035. [CrossRef]
4. Rioja, N. Estudio de la Degradación Fotocatalítica de Contaminantes Emergentes: Desarrollo de Composites Fotoactivos y Aplicación en un Reactor de Spouted Bed. Ph.D. Thesis, Universidad de Navarra, Pamplona, Spain, 2015.
5. Villota, N.; Ferreiro, C.; Qulatein, H.A.; Lomas, J.M.; Camarero, L.M.; Lombraña, J.I. Colour Changes during the Carbamazepine Oxidation by Photo-Fenton. *Catalysts* **2021**, *11*, 386. [CrossRef]
6. Villota, N.; Ferreiro, C.; Qulatein, H.A.; Lomas, J.M.; Lombraña, J.I. Turbidity Changes during Carbamazepine Oxidation by Photo-Fenton. *Catalysts* **2021**, *11*, 894. [CrossRef]
7. Ferrari, B.; Paxéus, N.; Giudice, R.; Pollio, A.; Garric, J. Ecotoxicological Impact of Pharmaceuticals Found in Treated Wastewaters: Study of Carbamazepine, Clofibric Acid, and Diclofenac. *Ecotoxicol. Environ. Saf.* **2003**, *55*, 359–370. [CrossRef]

8. Jos, A.; Repetto, G.; Rios, J.C.; Hazen, M.J.; Molero, M.L.; del Peso, A.; Salguero, M.; Fernández-Freire, P.; Pérez-Martín, J.M.; Cameán, A. Ecotoxicological Evaluation of Carbamazepine Using Six Different Model Systems with Eighteen Endpoints. *Toxicol. Vitr.* **2003**, *17*, 525–532. [CrossRef] [PubMed]
9. Van den Brandhof, E.J.; Montforts, M. Fish Embryo Toxicity of Carbamazepine, Diclofenac and Metoprolol. *Ecotoxicol. Environ. Saf.* **2010**, *73*, 1862–1866. [CrossRef] [PubMed]
10. Cummings, C.; Stewart, M.; Stevenson, M.; Morrow, J.; Nelson, J. Neurodevelopment of Children Exposed in utero to Lamotrigine, Sodium Valproate and Carbamazepine. *Arch. Dis. Child.* **2011**, *96*, 643–647. [CrossRef] [PubMed]
11. Atkinson, D.E.; Brice-Bennett, S.; D'Souza, S.W. Antiepileptic Medication During Pregnancy: Does Fetal Genotype Affect Outcome? *Pediatr. Res.* **2007**, *62*, 120–127. [CrossRef]
12. Gioia, R.; Dachs, J. The Riverine Input–Output Paradox for Organic Pollutants. *Front. Ecol. Environ.* **2012**, *8*, 405–406. [CrossRef]
13. Zhang, L.; Zhao, X.; Niu, C.; Tang, N.; Guo, H.; Wen, X.; Liang, C.; Zeng, G. Enhanced Activation of Peroxymonosulfate by Magnetic Co_3MnFeO_6 Nanoparticles for Removal of Carbamazepine: Efficiency, Synergetic Mechanism and Stability. *Chem. Eng. J.* **2019**, *362*, 851–864. [CrossRef]
14. Writer, J.H.; Antweiler, R.C.; Ferrer, I.; Ryan, J.N.; Thurman, E.M. In-Stream Attenuation of Neuro-Active Pharmaceuticals and Their Metabolites. *Environ. Sci. Technol.* **2013**, *47*, 9781–9790. [CrossRef]
15. Yamamoto, H.; Nakamura, Y.; Moriguchi, S.; Nakamura, Y.; Honda, Y.; Tamura, I.; Hirata, Y.; Hayashi, A.; Sekizawa, J. Persistence and Partitioning of Eight Selected Pharmaceuticals in the Aquatic Environment: Laboratory Photolysis, Biodegradation and Sorption Experiments. *Water Res.* **2009**, *43*, 351–362. [CrossRef] [PubMed]
16. Till, A.E. Pharmaceutical Data Elude Researchers. *Environ. Sci. Technol.* **2005**, *39*, 392A. [CrossRef] [PubMed]
17. Al Aukidy, M.; Verlicchi, P.; Jelic, A.; Petrovic, M.; Barcelò, D. Monitoring Release of Pharmaceutical Compounds: Occurrence and Environmental Risk Assessment of Two WWTP Effluents and Their Receiving Bodies in the Po Valley, Italy. *Sci. Total Environ.* **2012**, *438*, 15–25. [CrossRef]
18. Christoffels, E.; Brunsch, A.; Wunderlich-Pfeiffer, J.; Mertens, F.M. Monitoring Micropollutants in the Swist River Basin. *Water Sci. Technol.* **2016**, *74*, 2280–2296. [CrossRef]
19. Kinney, C.A.; Furlong, E.T.; Werner, S.L.; Cahill, J.D. Presence and Distribution of Wastewater-Derived Pharmaceuticals in Soil Irrigated with Reclaimed Water. *Environ. Toxicol. Chem.* **2006**, *25*, 317–326. [CrossRef]
20. Aldeguer, A. Tratamientos Combinados de Carbón Activado y Ozono Para Reducir la Presencia de Atrazina, Simazina, Carbamazepina y Diclofenaco en Medio Acuoso. Ph.D. Thesis, Universidad de Alicante, Alicante, Spain, 2022.
21. Vogna, D.; Marotta, R.; Napolitano, A.; Andreozzi, R.; D'Ischia, M. Advanced Oxidation of the Pharmaceutical Drug Diclofenac with UV/H_2O_2 and Ozone. *Water Res.* **2004**, *38*, 414–422. [CrossRef]
22. Rivera-Jaimes, J.A.; Postigo, C.; Melgoza-Alemán, R.M.; Aceña, J.; Barceló, D.; López de Alda, M. Study of Pharmaceuticals in Surface and Wastewater from Cuernavaca, Morelos, Mexico: Occurrence and Environmental Risk Assessment. *Sci. Total Environ.* **2018**, *613–614*, 1263–1274. [CrossRef]
23. Tran, N.; Drogui, P.; Brar, S.K. Sonoelectrochemical oxidation of carbamazepine in waters: Optimization using response surface methodology. *J. Chem. Technol. Biotechnol.* **2015**, *90*, 921–929. [CrossRef]
24. Darabi, K.; Azhdarpoor, A.; Dehghani, M. Evaluation of carbamazepine removal from aqueous medium using a combined method of ozonation and calcium alginate immobilized Aspergillus niger. *Biomass Convers. Biorefin.* **2024**, *14*, 3513–3522. [CrossRef]
25. Saeid, S.; Kråkström, M.; Tolvanen, P.; Kumar, N.; Eränen, K.; Mikkola, J.-P.; Kronberg, L.; Eklund, P.; Peurla, M.; Aho, A.; et al. Advanced oxidation process for degradation of carbamazepine from aqueous solution: Influence of metal modified microporous, mesoporous catalysts on the ozonation process. *Catalysts* **2020**, *10*, 90. [CrossRef]
26. Yacouba, Z.A.; Lesage, G.; Mendret, J.; Zaviska, F.; Petit, E.; Brosillon, S. Fate and toxicity of carbamazepine and its degradation by-products during coupling of ozonation and nanofiltration for urban wastewater reuse. *Front. Environ. Chem.* **2021**, *2*, 798785. [CrossRef]
27. *ISO 7027-1:2016*; Water Quality—Determination of Turbidity—Part 1: Quantitative Methods. International Organization for Standardization (ISO): Geneva, Switzerland, 2016.
28. Shangguan, Q.; DeGrandpre, M.D.; Hall, R.O., Jr.; Payn, R.A. Freshwater Carbonate Buffering Revisited. *Limnol. Oceanogr. Lett.* **2025**, *10*, 619–635. [CrossRef]
29. Asakai, T.; Maksimov, I.; Onuma, S. Batch-to-Batch Reproducibility for the Primary pH Method for Carbonate Buffer Solutions. *Anal. Bioanal. Chem.* **2024**, *416*, 3261–3269. [CrossRef]
30. Duoandicoechea, U.; González-Nogales, N.S.; Villota, N. Ozonation Efficiency in the Removal of Sulfamethoxazole from Water: Role of Mass Transfer and pH Effect in the Kinetic Analysis. *Ind. Eng. Chem. Res.* **2025**, *64*, 14459–14466. [CrossRef]

Disclaimer/Publisher's Note: The statements, opinions and data contained in all publications are solely those of the individual author(s) and contributor(s) and not of MDPI and/or the editor(s). MDPI and/or the editor(s) disclaim responsibility for any injury to people or property resulting from any ideas, methods, instructions or products referred to in the content.